Synthesis and docking studies of some novel heterocyclic moieties acting as superior inhibitors

Sujatha G.[1], Pazhanisamy T.[1], Suresh M.[2] and Ramanathan P.[1*]
1. PG and Research Department of Chemistry, Thanthai Hans Roever College (Autonomous), (Affiliated to Bharathidasan University), Perambalur - 621220, Tamil Nadu, INDIA
2. Department of Chemistry, AVS College of Arts and Science (Autonomous), (Affiliated to Periyar University), Salem – 636 106, Tamil Nadu, INDIA
*ramanathanp2010@gmail.com

Abstract

We created new xanthene derivatives in this study for the traditional approach and the derivatives validity is supported by mass spectral, NMR and infrared imaging methods. In the current situation, the virus has been affecting a large number of people worldwide for the last two years. Docking studies were conducted to explore the potential binding mechanism of the target compounds and xanthene derivatives were used in the prediction of molecular docking for novel compounds. The lowest binding energies, which were verified by protein binding to the compounds, were -5.43, -5.57, -6.25, -5.99 and -5.47 kcal/mol, appropriate binding confirmation for the docking validates the hydrogen bonding interactions. Compound 3 molecular researches revealed that the three main interactions involving this ligands attachment to the SARS-CoV-2 acceptor are the presence of hydrogen bonds, hydrophobic contacts and moderate polar interactions.

The docked compound 3 two-dimensional interaction diagram showed that hydrophobic residues like CYSA:42 and HISA:101 surround the ligand. This observation led to the conclusion that the binding process involves both de-solvation effects and hydrophobic contacts. Moreover, the target ligand 3 surface is surrounded by hydrophilic residues such as THRA:41, GLYA:40, PROA:10, ASPA:39, SERA:8 and LEUA:37. Compound 3 (para-methoxy substituted) among the synthesised compounds 1-6 exhibited a good docking score of -6.25 and binding energy of -4.60 kcal/mol. Compound 3 appears to have superior ligand-protein interactions while the remaining moieties show only moderate activity in docking tests.

Keywords: IR, NMR, Molecular Docking, H –Bonding, Binding energy

Introduction

Molecular docking is an optimisation problem that uses the "best-fit" orientation of a ligand that binds to a certain protein of interest to forecast the shape of the intermolecular complex formed between two or more molecules. The protein-ligand interaction is the most intriguing example due to its medical uses[1]. To better understand drug-receptor interactions, molecular docking is a common tool in modern drug design. Globally, invasive microbial infections are a serious issue, particularly for individuals with weakened immune systems. Since antimicrobial resistance has grown in this century, it is necessary to create new antimicrobial agents that are less toxic, more potent and more selective than the ones now used in clinical therapy. It is discovered that heterocycles with an azole ring system display a variety of biological activities such as antifungal and antibacterial qualities[2]. The pharmacological properties of imidazole derivatives are widely varied and include anti-inflammatory, analgesic, anti-convulsant, antitubercular, antibacterial and anticancer properties[3-5]. Significant biological activity has been demonstrated by pyrazole derivatives which has greatly accelerated the hunt for possible pharmacologically active medications that contain pyrazole substituents[6–11].

Numerous types of chemicals' antimicrobial activity suggested the presence of specific pharmacophores like imidazole and pyrazole[12,13]. The six physiologically active moieties' docking studies help us to understand how drugs interact with receptors. To forecast the ligand-protein predominant binding mechanisms, molecular docking experiments were performed. In order to find effective scaffolds that can be further developed into medications, the molecular docking study of the moieties was analysed.

Material and Methods

Synthetic route of xanthene derivatives: 5,5-dimethylcyclohexane-1,3-dione, acetic acid medium and substituted benzaldehyde combined benzene and ethyl acetate (9:1) were used as the eluent during the six hours that the reaction mixture was refluxed and the reaction's completion was tracked using the TLC technique. Column chromatography was utilised to purify the resulting substance. Scheme 1 shows the schematic representation of the synthesis mechanism of xanthene derivatives (1-6).

Spectral Measurements: Using a Bruker AMX 400 MHz NMR spectrometer, the ^{1}H and ^{13}C NMR spectra of the synthesised compounds in DMSO were captured. Using KBr pellets, infrared spectra were captured on a JASCO FT-IR-5300 spectrometer between the 4000 – 400 cm^{-1} range.

Molecular docking Studies: Using Argus Lab 4.0, a molecular docking simulation was carried out. The 3D structures that were ready were obtained from the protein data library and the option labelled "Making binding site for this protein" occurred to create the binding site.

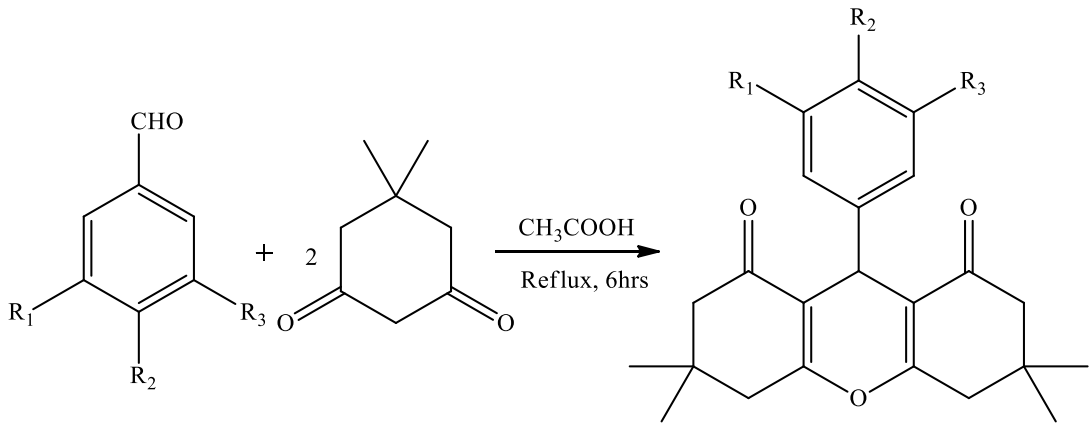

R_1 = H, -OCH_3, H, -OCH_3, H and H
R_2 = -CH_3, -OH, -OCH_3, -OCH_3, -Cl and -N-$(CH_3)_2$
R_3 = H, -OCH_3, -OH, -OCH_3, H and H

Scheme 1: Synthetic route of xanthene derivatives

Following the introduction of the ligand, the search method and scoring mechanism based on shapes were used to allow the docking calculation to proceed. The assessment of the energy between the ligand and the protein target is the responsibility of the scoring function. Flexible docking was enabled by creating grids over the protein binding sites and providing energy-based rotation for the ligand group of atoms without rotatable links. The hydrogen bond interaction between the ligand and protein near the substrate binding site determined the most suitable binding conformation and arguslab's lowest binding energy was used to select the best docking model.

The highest binding affinity is associated with the lowest energy poses because excessive energy leads to unstable conformations. The finished receptor model and the 2D and 3D interactions may both be viewed in Discovery Studio 4.5 versions, thanks to its storage in a Brookhaven PDB file.

Results and Discussion

Spectral Data

Compound (1): M.F.: $C_{24}H_{28}O_3$: IR (cm^{-1}); 1663.60 (C=O); 3037.87 – 2874.79 (Aromatic C-H); 1625.26 (C=C) (Figure 1). ^{1}H NMR (DMSO, ppm); δ: 7.04 (dd, 9.20 MHz, 4H), 0.89 (s, 6H), 1.03 (s, 6H), 2.23 (s, 3H (C23 Protons)), 2.08 (s, 4H), 2.51 (s, 4H), 4.47 (s, 1H) (Figure 2). ^{13}C NMR (DMSO, ppm); δ: 20.95, 26.74, 29.14, 31.22, 32.27, 38.93, 50.45, 114.96, (128.38, 128.93, 135.78, 141.75, 163.52 for aromatic carbons), 197.06 (C=O) (Figure 3).

Compound (2): M.F.: $C_{25}H_{30}O_6$: IR (cm^{-1}); 1661.67 (C=O); 3012.74 – 2871.98 (Aromatic C-H); 1617.09 (C=C). ^{1}H NMR (DMSO, ppm); δ: 0.87 (s, 6H, CH_3), 1.00 (s, 6H, CH_3), 2.07 (s, 4H), 2.50 (s, 4H), 3.64 (s, 1H), 4.01 (s, 6H for methoxy groups), 6.34 (s, 1H (C23 – for OH - group)), 8.38 (s, 12H for aromatic protons) ^{13}C NMR (DMSO, ppm); δ: 26.69, 29.26, 31.19, 32.31, 50.54, (56.42 for methoxy carbons (C21, 22)), 106.17, 115.04, (134.63, 134.99, 147.94, 163.22, Aromatic carbons), 196.66 (C=O).

Compound (3): M.F.: $C_{24}H_{28}O_5$: IR (cm^{-1}); 1666.00 (C=O); 2955.56 – 2896.74 (Aromatic C-H); 1626.13 (C=C). ^{1}H NMR (DMSO, ppm); δ: 0.92 (s, 6H), 1.03 (s, 6H), 2.28 (s, 2H), 2.10 (s, 2H), 2.51 (s, 4H), 3.68 (s, 3H), 4.38 (s, 1H), 6.64 (d, J=1.6Hz, 1H), 6.73 (d, J=8.4Hz, 1H), 8.80 (s, 1H for hydroxyl group). ^{13}C NMR (DMSO, ppm); δ: 26.97, 29.16, 30.72, 32.32, 50.54, (55.93 for –OCH_3 carbon (C23)), 112.05, 115.15, 116.22, 118.90, (137.43, 146.23, 146.40, 163.03 for aromatic carbons), 196.57 (C=O).

Compound (4): M.F.: $C_{26}H_{32}O_6$: IR (cm^{-1}); 1667.68 (C=O); 2954.84 – 2876.42 (Aromatic C-H); 1625.29 (C=C). ^{1}H NMR (DMSO, ppm); δ: 0.92 (s, 6H), 1.04 (s, 6H), 2.07 (s, 4H), 2.25 (s, 4H), 3.67 (s, 9H for -OCH_3 protons), 4.46 (s, 1H), 6.72 (s, 2H). ^{13}C NMR (DMSO, ppm); δ: 27.5, 32.3, 38.9, 39.6, 51.5, 56.1, 60.8, 106.4, 113.9, 136.2, 136.5, 152.8, 155.0, 198.9.

Compound (5): M.F.: $C_{23}H_{25}ClO_3$: IR (cm^{-1}); 1661.59 (C=O); 2953.05 – 2875.23 (Aromatic C-H); 1626.18 (C=C). ^{1}H NMR (DMSO, ppm); δ: 0.89 (s, 6H), 1.03 (s, 6H), 2.05 (s, 2H), 2.25 (s, 2H), 2.51 (s, 4H), 4.49 (s, 1H), 7.18 (d, J=8.4Hz, 2H), 7.28 (d, J=8.4Hz, 2H). ^{13}C NMR (DMSO, ppm); δ: 26.94, 29.07, 31.41, 32.32, 50.43, 114.42, (128.30, 130.39, 131.19, 143.72 for aromatic carbons), 163.60, 196.65 (C=O).

Compound (6): M.F.: $C_{25}H_{31}NO_3$: IR (cm^{-1}); 1660.70 (C=O); 2965.62 – 2872.99 (Aromatic C-H); 1611.07 (C=C). ^{1}H NMR (DMSO, ppm); δ: 0.89 (s, 6H), 1.03 (s, 6H), 2.08 (s, 4H), 2.51 (s, 4H), 3.06 (s, 6H for –CH_3 protons), 4.47 (s, 1H), 6.94 (d, J=8.0Hz, 2H), 7.14 (d, J=9.5Hz, 2H). ^{13}C NMR (DMSO, ppm); δ: 26.34, 28.08, 32.62, 45.86, 50.43, 112.05, 113.31, (120.56, 136.33, 146.40 for aromatic carbons), 163.03, 189.17 (C=O).

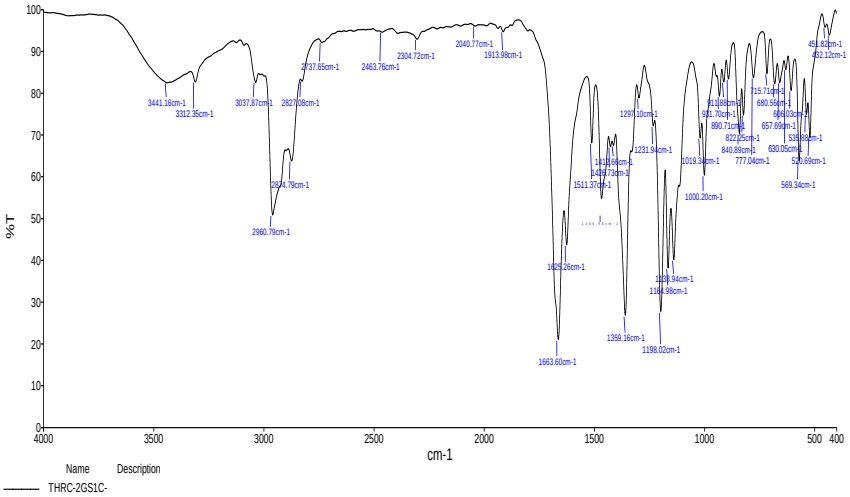

Figure 1: Representative FT-IR spectrum of compound 1

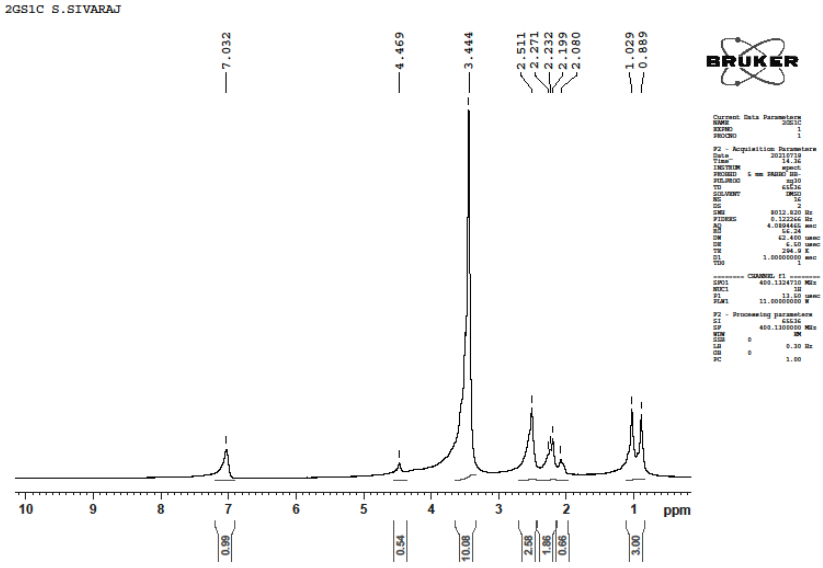

Figure 2: Representative ^{1}H NMR spectrum of compound 1

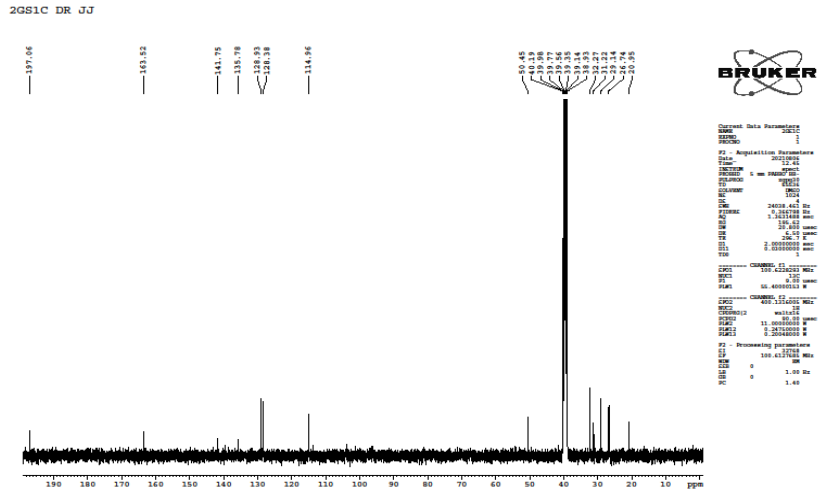

Figure 3: Representative ^{13}C NMR spectrum of compound 1

Molecular Docking studies: Flexible protein-ligand docking is carried out throughout the docking computations, which look for advantageous interactions between one, usually tiny, ligand molecule and one, usually larger, protein molecule. There are three processes involved in the docking procedure. 20 poses are used in this refining process limited by protein preparation. If the ligand poses are within 5.0 Å, prime induced fit occurs wherein the side chains are optimized and residues are refined. It consists of using conventional precision mode to do the gliding re-docking stage. Three factors were taken into consideration while selecting the optimum docked structure: glide score function, glide energy and the quantity of amino acid matches (hydrogen bonds) with the reference medication.

Compound binding interaction is observed with active site residues (Figure 4) (Crystal Structure of NSP1 from SARS-CoV-2, PDB ID: 7K3N). Compound 3 molecular researches revealed that the three main interactions involving this ligand's attachment to the SARS-CoV-2 acceptor are the presence of hydrogen bonds, hydrophobic contacts and moderate polar interactions. Figure 5 displays the hydrophilic and hydrophobic two-dimensional interactions. The docked compound 3 two-dimensional interaction diagram showed that hydrophobic residues like CYSA:42 and HISA:101 surround the ligand. This observation led to the conclusion that the binding process involves both desolvation effects and hydrophobic contacts. The target ligand 3's surface is also surrounded by hydrophilic residues such as THRA:41, GLYA:40, PROA:10, ASPA:39, SERA:8 and LEUA:37. Hence, these hydrophilic residues also improve binding affinities.

The π-π stacking interactions between the protein and the ligand binding site residue in compound 3 unexpectedly improve the binding interactions much further. Compound 3 (para-methoxy substituted) among the synthesised compounds 1-6 exhibited a good docking score of -6.25 and binding energy of -4.60 kcal/mol. Compound 3 appears to exhibit superior ligand-protein interactions whereas the remaining moieties demonstrate intermediate docking study activity. Table 1 lists the protein hydrophilic and hydrophobic interactions with compounds 1-6 as well as its docking score and H bonding energy.

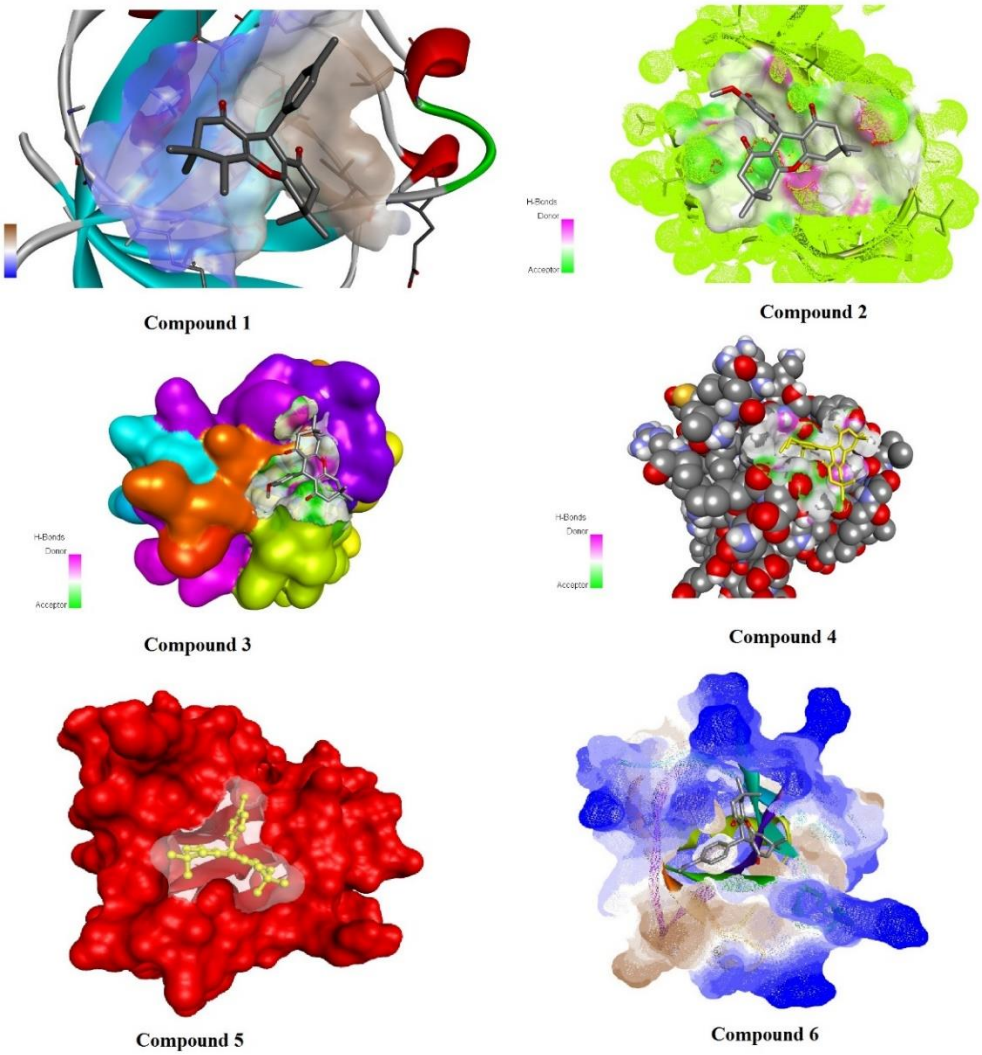

Figure 4: 3D Binding interactions of 1-6 with active site residues of 7K3N receptor

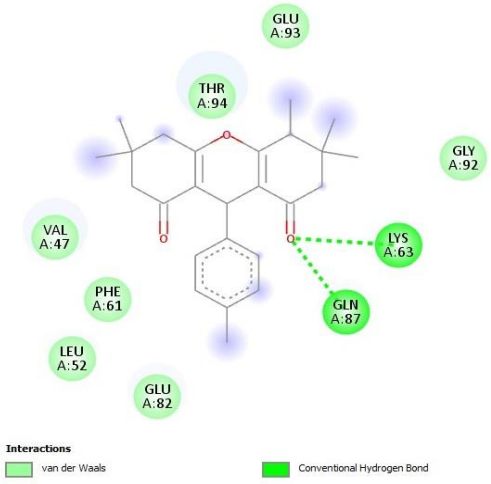

Compound 1

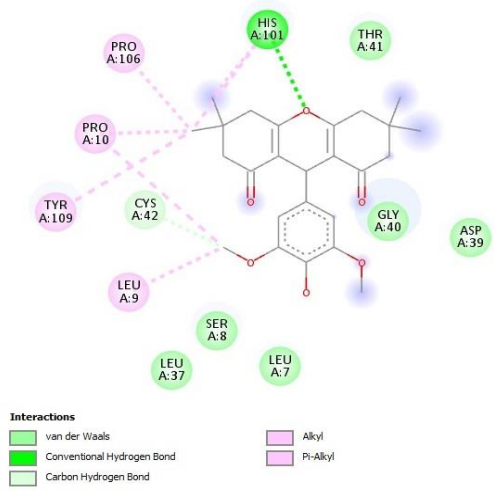

Compound 2

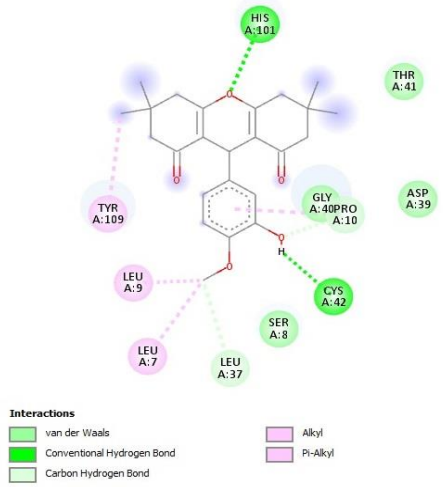

Compound 3

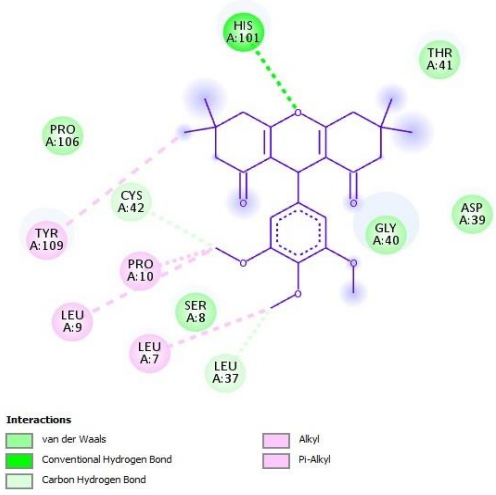

Compound 4

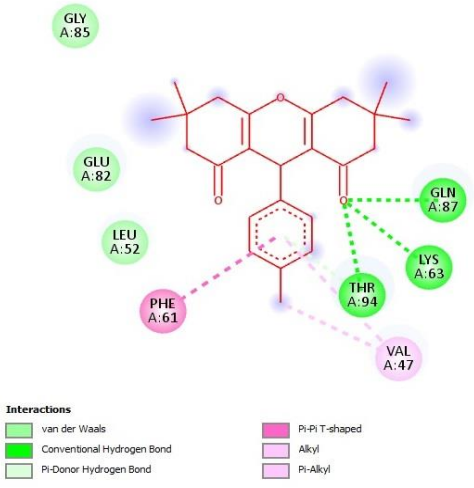

Compound 5

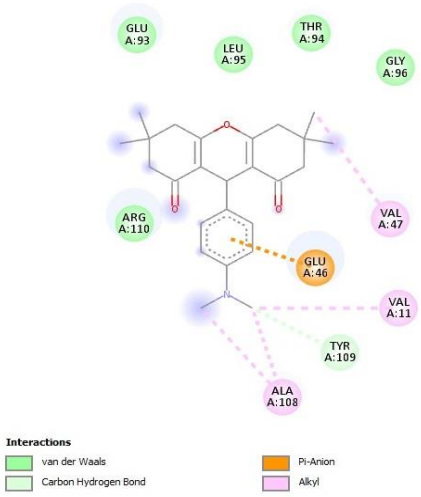

Compound 6

Figure 5: Hydrophilic and hydrophobic interactions of the compound 1-6

Table 1
Docking score, H-bonding energy, binding energy and interactions between molecules 1-6 that are hydrophilic and hydrophobic

Compds.	Docking score	H – bonding energy (kcal/mol)	Combining energy (kcal/mol)	Residues of hydrophobic interactions	Residues of hydrophilic interactions
1	-5.43	-4.82	-5.13	LYSA:63, GLNA:87	THRA:94, GLUA:93, GLYA:92, VALA:47, PHEA:61, LEUA:52, GLUA:82
2	-5.59	-3.51	-3.48	HISA:101	THRA:41, CYSA:42, GLUA:40, ASPA:39, SERA:8, LEUA:37, LEUA:7
3	-6.25	-5.28	-4.60	HISA:101, CYSA:42	THRA:41, GLYA:40, PROA:10, ASPA:39, SERA:8, LEUA:37
4	-5.69	-4.72	-4.85	HISA:101,	THRA:41, GLYA:40, PROA:106, ASPA:39, SERA:8, LEUA:37
5	-5.99	-3.80	-3.43	THRA:94, LYSA63, GLNA:87	GLYA:85, GLUA:82, LEUA:52
6	-5.47	-5.15	-5.17	GLUA:46	GLUA:93, LEUA:95, THRA:94, GLYA:96, ARGA:110

Conclusion

Six novel xanthene compounds were synthesised and characterised using mass spectrometry, IR spectroscopy and NMR. Docking studies were conducted to explore the potential binding mechanism of the target compounds and xanthene derivatives were used in the prediction of molecular docking for novel compounds. The lowest binding energies, which were verified by protein binding to the compounds, were -5.43, -5.57, -6.25, -5.99 and -5.47 kcal/mol.

Compound 3 (para-methoxy substituted) among the synthesised compounds 1-6 exhibited a good docking score of -6.25 and binding energy of -4.60 kcal/mol. Compound 3 appears to have superior ligand-protein interactions while the remaining moieties show only moderate activity in docking tests.

Acknowledgement

We would especially like to thank Mr. M. Santhosh Kumar, Research Scholar at Thiruvalluvar University in Vellore for his assistance with the biological activities. We thank Mr. S. Sivaraj, Research Scholar, Department of Chemistry, Annamalai University for assistance with the NMR facility. We would also like to thank St. Joseph College, Tiruchirappalli for lending their IR facilities.

References

1. Arthington-Skaggs B.A., Motley M., Warnock D.W. and Morrison C.J., *J. Clinical Microbiol.*, **38**, 2254 **(2000)**

2. Bekhita A.A. and Abdel-Aziem T., *Bioorg. Med. Chem.*, **12**, 1935 **(2004)**

3. Borowski E., *Farmaco*, **55**, 206 **(2000)**

4. Chmara H., Andruszkiewicz R. and Borowski E., *Biochem. Biophys. Res. Commun*., **120**, 865 **(1984)**

5. Dhanya S., Isloor A.M. and Shetty P., *Der. Pharma Chemica.*, **1**, 19 **(2009)**

6. Isloor A.M., Kalluraya B. and Rao M., *J. Saudi Chem. Soc.*, **4**, 265 **(2000)**

7. Isloor A.M., Kalluraya B. and Shetty P., *Eur. J. Med. Chem.*, **44**, 3784 **(2009)**

8. Leema Rose A., Janeeta Priya F., Vidhya S. and Amsica T.R., *Res. J. Biotech.*, **18(11)**, 58 **(2023)**

9. Milewski S., Chmara H. and Borowski E., *Arch. Microbiol*., **145**, 234 **(1986)**

10. Miyachi H., Kiyota H. and Segawa M., *Bioorg. Med. Chem. Lett.*, **8**, 1807 **(1998)**

11. Morris G.M., Goodsell D.S., Halliday R.S., Huey R., Hart W.E., Belew R.K. and Olson A.J., *J. Comput. Chem.*, **19**, 1639 **(1998)**

12. Mouilleron S., Badet-Denisot M.A. and Golinelli-Pimpaneau B., *J. Mol. Biol.*, **377(4)**, 1174 **(2008)**

13. Pandey J., Tiwari V.K., Verma S.S., Chaturvedi V., Bhatnagar S., Sinha S., Gaikwad A.N. and Tripathi R.P., *Eur. J. Med. Chem.*, **44**, 3350 **(2009)**

14. Pinza M., Farina Z., Cerri A., Pfeiffer U., Riccaboni M.T., Banfi S., Biagetti R., Pozzi O., Magnani M. and Dorigotti L., *J. Med. Chem.*, **36**, 4214 **(1993)**

15. Sander T., Freyss J., Korff M.V., Reich J.R. and Rufener C., *J. Chem. Info.Model*., **49**, 232 **(2009)**

16. Schuttelkopf A.W. and Aalten D.M.F.V., *Acta Crystallo*., **D60**, 1355 **(2004)**

17. Sharma N.K., Jha K.K. and Priyanka J., *J. Adv. Sci. Res.*, **1**, 67 **(2010)**

18. Suzuki F., Kuroda T., Tamura T., Sato S., Ohmori K. and Ichikawa S., *J. Med. Chem.*, **35**, 2863 **(1992)**

19. Vijesh A.M., Isloor A.M., Telkar S., Peethambar S.K., Rai S. and Isloor N., *Eur. J. Med. Chem.*, **46**, 3531 **(2011)**.

(Received 31st January 2024, accepted 04th April 2024)